Electrochimica Acta 153 (2015) 583–593

Contents lists available at ScienceDirect

Electrochimica Acta

journal homepage: www.elsevier.com/locate/electacta

N-type Cu_2O Film for Photocatalytic and Photoelectrocatalytic Processes: Its stability and Inactivation of *E. coli*

Liangbin Xiong [a,b], Tsz Wai Ng [a], Ying Yu [c,*], Dehua Xia [a], Ho Yin Yip [a], Guiying Li [d], Taicheng An [d], Huijun Zhao [e], Po Keung Wong [a,**]

[a] School of Physics and Electronic-Information Engineering, Hubei Engineering University, Xiaogan, 432100, China
[b] School of Life Sciences, The Chinese University of Hong Kong, Shatin, NT, Hong Kong SAR, China
[c] Institute of Nanoscience and Nanotechnology, College of Physical Science and Technology, Central China Normal University, Wuhan 430079, China
[d] State Key Laboratory of Organic Geochemistry, Guangzhou Institute of Geochemistry, Chinese Academy of Sciences, Guangzhou, 510640, China
[e] Centre for Clean Environment and Energy, and Griffith School of Environment, Gold Coast Campus, Griffith University, Queensland, 4222, Australia

ARTICLE INFO

Article history:
Received 26 September 2014
Received in revised form 24 November 2014
Accepted 26 November 2014
Available online 27 November 2014

Keywords:
Cu_2O
photoelectrocatalytic inactivation
charge transfer
Escherichia coli
reactive oxygen species
membrane-separated reactor

ABSTRACT

Photoelectrocatalytic (PEC) inactivation of *Escherichia coli* K-12 by cuprous oxide (Cu_2O) film irradiated by visible light is firstly reported. A complete inactivation of about 7 log of *E. coli* was obtained for Cu_2O film within 6 h. The bacterial inactivation efficiency was significantly improved in a photoelectrochemical cell, in which 7 log of *E. coli* could be completely inactivated within 2 h by Cu_2O film with a 0.1 V bias. Electric charge transfer between electrodes and *E. coli*, and electric charge inactivation towards *E. coli* were investigated using membrane-separated reactor combined with short circuit photocurrent technique. H_2O_2, hole, and toxicity of Cu_2O film were found responsible for the inactivation of *E. coli*. Toxicity of copper ions (including Cu^{2+} and Cu^{+}) leakage from Cu_2O films was determined and the results showed that the amount of leakage copper ions was not toxic to *E. coli*. Finally, the Cu_2O film was proved to be effective and reusable for PC and PEC inactivation of *E. coli*.

1. INTRODUCTION

The n-type Cu_2O has attracted much attention recently owing to its higher photoactivity than p-type counterpart [1] and potential application for homojunction solar cells or photoelectrochemical cell [2]. N-type film invariably gives better photoactivity than the p-type film since holes with a lower mobility than electrons, are very likely to be lost in e^{-}-h^{+} recombination [3]. Cu_2O is also a good antimicrobial material [4] and even found to have crystallographic facet-dependent antibacterial activity [5,6], and Cu_2O based composites (Cu_2O/ZnO [7], Cu_2O-CuO/$Sr_3BiO_{5.4}$ [8], Cu_2O/mineral wool fiber [9], Cu_2O/TiO_2 [10]) are widely reported for PC disinfection. However, there is no report on photocatalytic (PC) bacterial inactivation by pristine Cu_2O except a preliminary study by our group [11]. Thus, we initiate an investigation on PC and PEC bacterial inactivation by pristine n-type Cu_2O.

Investigation on direct electron transfer between microbes and an electrode was first attempted in the early work of Matsunaga et al. [12], who contributed the death of microbes to its direct oxidation by TiO_2/Pt powder [13]. Their work was the center of attention in the field of PC and photoelectrocatalytic (PEC) inactivation of microbes, but work on electric charge transfer between microbes and a photoelectrode was very limited. In this study, electric charge transfer between *Escherichia coli* K-12 (*E. coli*) and Cu_2O film was investigated by PEC membrane-separated (PECMS) reactor incorporated with short circuit photocurrent (SCPC) technique [3,6]. The PECMS reactor is separated into two compartments by a semipermeable membrane which separates *E. coli* from Cu_2O film, or separates anode cell from cathode cell, convenient for independent investigations of inactivation of *E. coli* by Cu_2O, Pt, or reactive oxygen species (ROSs). Meanwhile, SCPC technique was used to monitor the charge transfer between an electrode and *E. coli*, and to investigate bacterial inactivation by electric charges of an electrode. To the best of our knowledge, no PECMS reactor combined with SCPC technique was introduced to date to study PEC bacterial inactivation.

Stability and reusability are the two most important factors for the feasibility of application of photocatalyst(s). Extensive reports

* Corresponding author. Tel.: +86 27 6786 7037; fax: +86 27 6786 1185.
** Corresponding author. Tel.: +852 3943 6383; fax: +852 2603 5767.
E-mail addresses: yuying@phy.ccnu.edu.cn (Y. Yu), pkwong@cuhk.edu.hk (P.K. Wong).

http://dx.doi.org/10.1016/j.electacta.2014.11.169
0013-4686/

on the stability of p-type Cu_2O film [14–16] and bulk [17–20] demonstrated that the morphology and phase compositions significantly effect on the stability of Cu_2O and the photocorrosion of Cu_2O leads to degradation of its PC property. However, study on the stability of n-type Cu_2O as a photocatalyst is of absence so far. Therefore, here, we carry out the measurement of the stability and reusability of n-type Cu_2O film via repeated cycling PC tests for bacterial inactivation.

Inactivation effect of Cu_2O film towards *E. coli* was observed under dark conditions, indicating that Cu_2O film can inactivate *E. coli*, not only in day time with light irradiation, but also at night. The low cost and environmentally benign nature of Cu_2O makes developing Cu_2O and Cu_2O-based photocatalysts very attractive. Moreover, the use of PECMS reactor combined with SCPC technique may promote more research interest in the investigation on photoelectrochemical bacterial inactivation.

2. EXPERIMENTAL SECTION

2.1. Materials

Copper sulfate ($CuSO_4 \cdot 5H_2O$, 98.0% purity) was obtained from Clyde (Australia). Copper foil (99.999% purity), sodium sulfate (99.0% purity), 2,3-bis(2-methoxy-4-nitro-5-sulfophehyl)-2H-tetrazolium-5-carboxanilide (XTT) (>98% purity), terephthalic acid (TA) (98% purity), horseradish peroxidase (POD) (activity: 250∼330 units/mg solid), N,N-diethyl-p-phenylenediamine (DPD) (97% purity), and bathocuproine disulfonic acid were received from Sigma-Aldrich. Nutrient agar (NA) and nutrient broth (NB) were purchased from Lab M (Lancashire, UK). All were used as purchased. The solutions used in this work were prepared with deionized water further purified with a Millipore Milli-Q (Millipore, Bedford, MA, USA) purification system (resistivity $\geq 18.2\,M\Omega$).

2.2. Preparation of Cu_2O film electrodes

The details of preparation of Cu_2O film can be found in our previous work [1]. A $1.5 \times 1.5\,cm^2$ golden copper foil shown in Fig. S1a in Supporting Information (SI) was immersed in 80 mL of 10^{-3} M copper sulfate aqueous solution in an autoclave. A brick-red Cu_2O film (Fig. S1b in SI) was prepared after the autoclave was kept in a temperature of 160 °C for 3 h.

2.3. PC and PEC reactors and light source

The schematic diagrams of the experimental reactors with about 100 mL of volume glass container homemade for PC and PEC regulation of *E. coli* are given in Fig. 1. There are four kinds of reactors: (a) PC reactor, in which Cu_2O film was dipped in suspension; (b) PEC reactor, in which Cu_2O film, Pt, and Ag/AgCl electrodes are used as working electrode, counter electrode, and reference electrode, respectively; (c) membrane-separated (MS) reactor, and (d) PEC membrane-separated (PECMS) reactor are the same as (a), (b), respectively, except that the reactors were separated into two compartments by a porous semipermeable membrane. The molecular weight cutoff of the semipermeable membrane is $12\sim14 \times 10^3$ dalton (pore size 5 nm), whereas the rod-shaped *E. coli* is about 2.6×10^6 dalton (size 500 nm), so that the direct contact was prohibited because *E. coli* cell cannot pass through the membrane [21]. The light source for photoelectrochemical characterizations and antibacterial tests was shown in

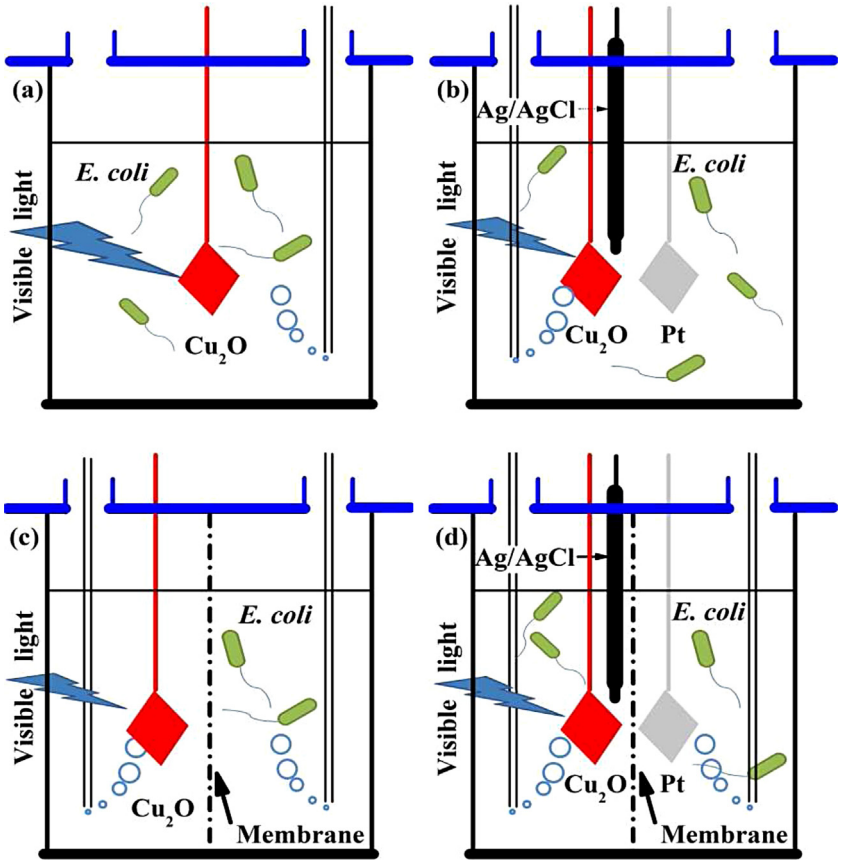

Fig. 1. Schematic diagrams of experimental reactors with about 100 mL of volume glass container for PC and PEC regulation of *E. coli*.

Fig. S2. A UV cutoff filter ($\lambda < 400$ nm) was used to ensure visible light (VL) irradiation. The light intensity was measured by a light meter (LI-COR, USA), and the light intensity for the experiments was fixed at 1200 mW/cm^2.

2.4. Characterization of Cu_2O film

XRD measurements were carried out on a PW 1840 powder X-ray diffractometer, using Cu Ka (1.54 Å) as the incident radiation. Scanning electron microscopy (SEM) images and were obtained on a field-emission scanning electron microscopy (FESEM, JEOL, JSM-6700F) at 30 kV. Energy dispersive X-ray spectrometry (EDX) (FESEM, OXFORD, INCA400) was carried out to characterize the composition of the samples. X-ray photoelectron spectroscopy (XPS) analyses of the samples were performed on a PHI-1600 ESCA spectrometer (USA) using 300 W Mg Kα radiation, and the binding energies were referenced to the C1s line at 285 eV from adventitious carbon. Photoelectrochemical characterization were conducted on a CHI660D electrochemical station (Chenhua, Shanghai) in 0.1 M air-saturated aqueous Na_2SO_4 solution with a three-electrode system (Cu_2O film as working electrode, Pt sheet (1.5×1.5 cm^2) as counter electrode, and KCl-saturated Ag/AgCl as reference electrode, respectively).

2.5. PC and PEC antibacterial test

The bacteria were cultured in nutrient broth (Lancashire, UK) at 37 °C and agitated at 200 rpm for 16 h. The culture was then washed twice with 0.1 M sterilized Na_2SO_4 solution by centrifugation at 5000 rpm for 5 min. The cell pellet was re-suspended in sterilized Na_2SO_4 solution and the cell density was finally adjusted to about 2×10^7 cfu/mL. Na_2SO_4 suspension of washed cells can be added into different reactors to conduct different antibacterial experiments. When antibacterial tests were conducted in PC, PEC and MS reactors, the reaction suspension was bubbled to ensure *E. coli* disperse well in solution by using an air pump throughout the experiments. When antibacterial test was conducted in PECMS reactor, argon gas was introduced at 150th s to bubble the suspension. At 2000th s, 1 mL of $\sim 10^8$ cfu/mL *E. coli* (about 2×10^7 cfu/mL in solution) was added to Cu_2O cell of PECMS reactor (Prior to the addition, the *E. coli* suspension was bubbled with Argon for at least 30 min). At different time intervals, aliquots of the sample were collected and serially diluted with sterilized Na_2SO_4 solution. 0.1 mL of the diluted sample was then immediately spread on nutrient agar (Lancashire, UK) plates and incubated at 37 °C for 24 h to determine the number of viable cells (in cfu). All antibacterial experiments were performed in triplicates.

2.6. Determination of the concentrations of copper ion

Cuprous ion (Cu^+) concentration was determined by colorimetric analysis using bathocuproine disulfonic acid, which selectively chelates Cu^+. Total copper ion concentration was also measured by the addition of ascorbic acid to reduce all of the cupric ions (Cu^{2+}) to Cu^+ [22]. The absorbance of the solution was measured at 457 nm using UV/Vis spectrophotometer (Blue Star A, US).

2.7. Detection of $^{\bullet}OH$, $^{\bullet}O_2^-$ and H_2O_2

Hydroxyl radical ($^{\bullet}OH$) was detected by a photoluminescence (PL) method by using TA as a probe molecule [23]. TA readily reacts with $^{\bullet}OH$ to produce a highly fluorescent product, 2-hydroxy-TA (TA-$^{\bullet}OH$), which was measured by an Infinite M200 fluorescence spectrophotometer (Tecan, Switzerland) at emission wavelength 425 nm with excitation wavelength at 315 nm. Experimental procedure was similar to the measurement of PC inactivation process in PC reactor except that the suspension was added with 0.4 μM TA and 2 μM NaOH. At different irradiation exposure times,

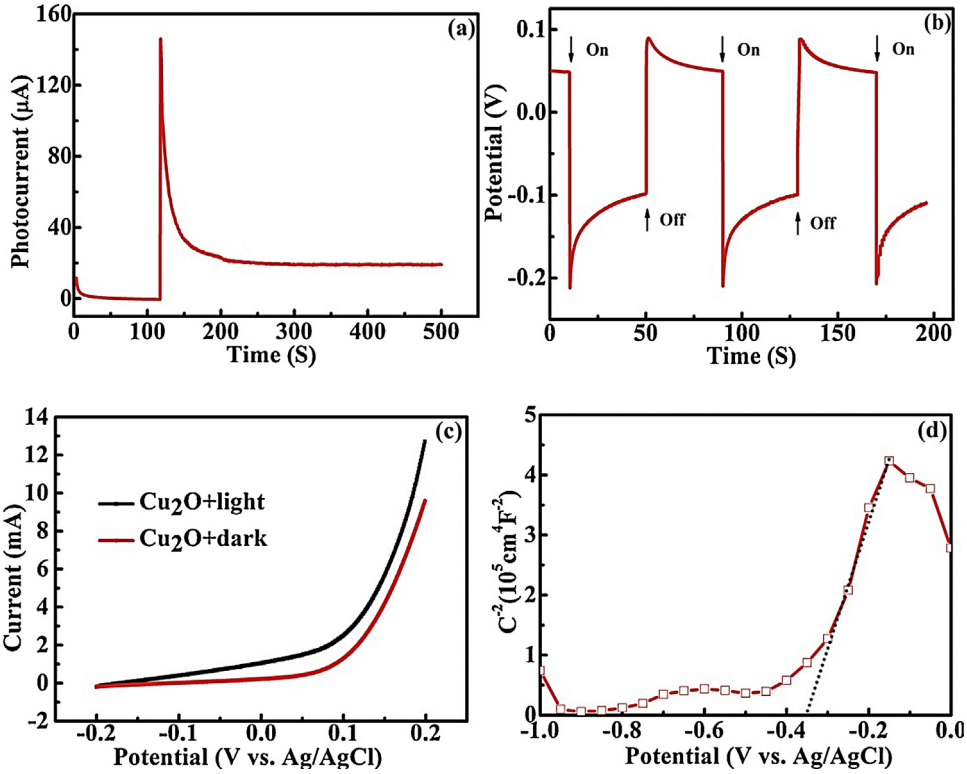

Fig. 2. Patterns of (a) SCPC of Cu_2O film under VL irradiation; (b) open circuit photovoltage of Cu_2O film measured under pulse irradiation; (c) linear sweep voltammogram for Cu_2O film under VL and dark, sweep rate 100 mVs^{-1}; and (d) Mott-Schottky plot of Cu_2O film; measured at 10 kHz, sweep rate 100 mVs^{-1}.

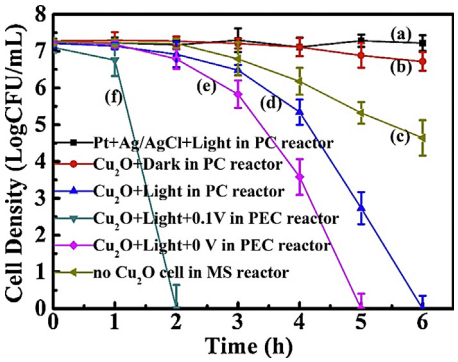

Fig. 3. Inactivation of *E. coli* (a) in PC reactor without Cu_2O film, but with Pt electrode and Ag/AgCl electrodes under light control; (b) by Cu_2O film in PC reactor under dark; (c) in no Cu_2O cell of MS reactor under VL; (d) by Cu_2O film in PC reactor under VL; (e) in PEC reactor with 0 V bias under VL; and (f) in PEC reactor with 0.1 V bias under VL.

1 mL of suspension was collected and filtered by centrifugation at 5000 rpm for 5 min at 25 °C, using the centrifuge (Hermle Z323, Germany) to remove *E. coli*. Superoxide radical ($^{\bullet}O_2^-$) was measured by XTT [24–26], which can be reduced by $^{\bullet}O_2^-$ to form XTT-formazan. The formazan has an absorption spectrum (measured by UV/Vis spectrophotometer (Blue Star A, US)) with a peak at 470 nm that can be used to quantify the relative amount of superoxide present. Experimental procedure was similar to the measurement of $^{\bullet}OH$ in PC reactor except that the 0.4 μM TA and 2 μM NaOH was replaced with 0.2 μM XTT. H_2O_2 was analyzed photometrically by the Peroxidase (POD)-catalyzed oxidation product of DPD [27,28], which was measured by UV/Vis spectrophotometer (Blue Star A, US)) at 551 nm.

2.8. Fluorescence spectroscopy

E. coli before and after PC treatment in PC reactor was collected and stained with the dyes of LIVE/DEAD BacLight bacterial viability kit (L7012, Molecular Probes, Inc. Eugene, OR) following the protocol recommended by the manufacture. After being incubated at 25 °C in the dark for 15 min, the samples were transferred to the coverslip and examined using a fluorescence microscopy (Nikon ECLIPSE 80i, Japan) equipped with a filter block NUV-2A consisting of excitation filter Ex 400–600 (Nikon, Japan) and Spot-K slider CCD camera (Diagnostic instruments. Inc. Sterling Heights, MI).

3. RESULTS AND DISCUSSION

3.1. Photoelectrochemical characterization

Fig. 2 displays the patterns of electrochemical and photoelectrochemical properties of freshly prepared Cu_2O film in 0.1 M Na_2SO_4. Fig. 2a shows an anode photocurrent response for Cu_2O film under irradiation, which is an n-type semiconductor behavior. The open circuit potential further confirms Cu_2O film electrode also have an n-type character for a negatively shifted potential response under irradiation (Fig. 2b). The current-potential curves (Fig. 2c) of the Cu_2O film under dark and irradiation were recorded

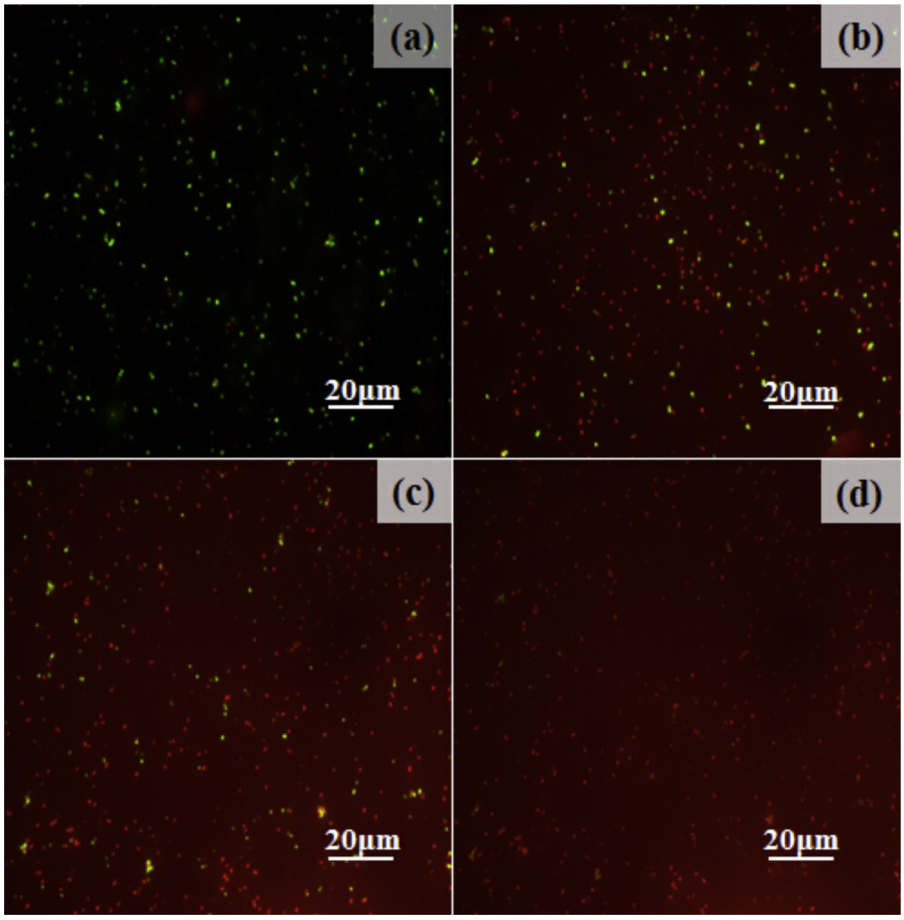

Fig. 4. Fluorescence microscopic images of *E. coli* (about 2×10^7 cfu/mL, 80 mL) photocatalytically untreated (a) or treated (b-d) in the presence of Cu_2O film in PC reactor with (a) 0 h (untreated *E. coli*), (b) 2 h, (c) 4 h, and (d) 6 h irradiation.

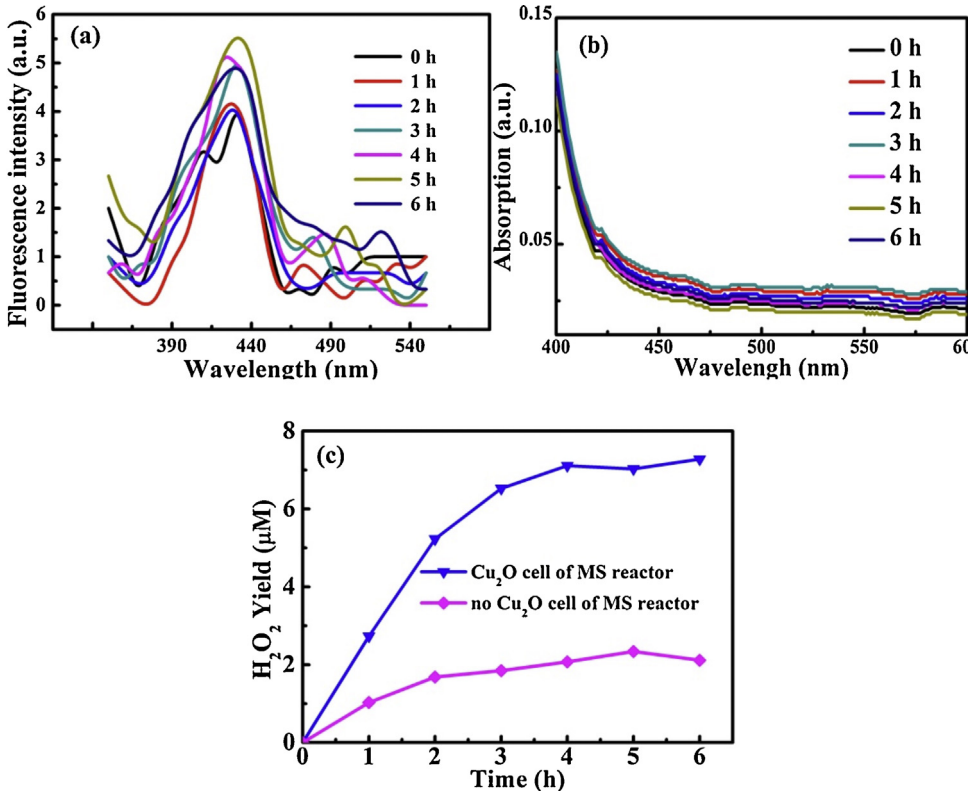

Fig. 5. (a) Fluorescence emission spectral changes for the filtrate from the suspension in PC reactor with Cu_2O film with 0.4 μM TA and 2 μM NaOH at different time under irradiation (excitation at 315 nm, emission at 425 nm); (b) absorption spectral changes of for the filtrate from the suspension in PC reactor with Cu_2O film and 200 μM XTT at different time under irradiation (absorption peak 470 nm); (c) H_2O_2 yield in Cu_2O cell of MS reactor, and no Cu_2O cell of MS reactor, respectively.

within the potential range −0.2 and +0.2 V (vs Ag/AgCl, the same below) at a potential sweep rate of 100 mVs^{-1}. The potential range from −0.2 V to +0.1 V, the Cu_2O film shows nearly perfect blocking characteristics, while an increase in dark current density for potential higher than +0.1 V is due to the oxidation of Cu_2O film (Fig. 2c). A significant increase in the anodic photocurrent density above −0.2 V occurred, indicating photogenerated carriers are generated and separated at the Cu_2O film electrode under irradiation. The anodic photocurrent appeared at −0.2 V suggests that the flatband potential of the Cu_2O film is blow −0.2 V. A more accurate position of the flatband potential was obtained by taking the x intercept of the Mott-Schottky plot of the Cu_2O film (Fig. 2d), which gave flatband potential of −0.35 V. The positive slope of the plot again proved the n-type nature of the Cu_2O film. The application of a potential over flatband potential can suppress charge carrier recombination resulting in extension of the lifetime of electrons and holes. Thus, a bias over −0.35 V on the n-type Cu_2O film electrode may improve the PEC efficiency. However, a negative bias on an n-type photoelectrode is not encouraged because of low efficiency and extra energy consumption whereas a positive bias on an n-type semiconductor electrode contributes to a highly PEC efficiency. Therefore, 0 and +0.1 V bias (positive enough but not result in oxidation of Cu_2O film) were chosen in photoelectrochemical experiments for the inactivation of *E. coli*.

3.2. PC and PEC inactivation

Fig. 3 shows the inactivation of *E. coli* under different conditions. Light control (Fig. 3a) shows the bacterial population remained essentially unchanged within 6 h, suggesting

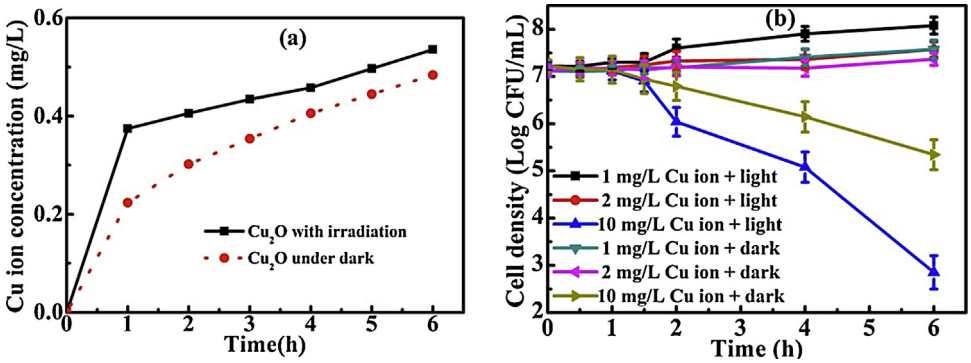

Fig. 6. (a) Concentrations of copper ion (leakage from Cu_2O films, including Cu^+ and Cu^{2+}) as a function of time when Cu_2O film immersed in 0.1 M Na_2SO_4 solution under irradiation and dark; (b) inactivation of *E. coli* in 0.1 M Na_2SO_4 solution with different concentrations of copper ion under irradiation and dark.

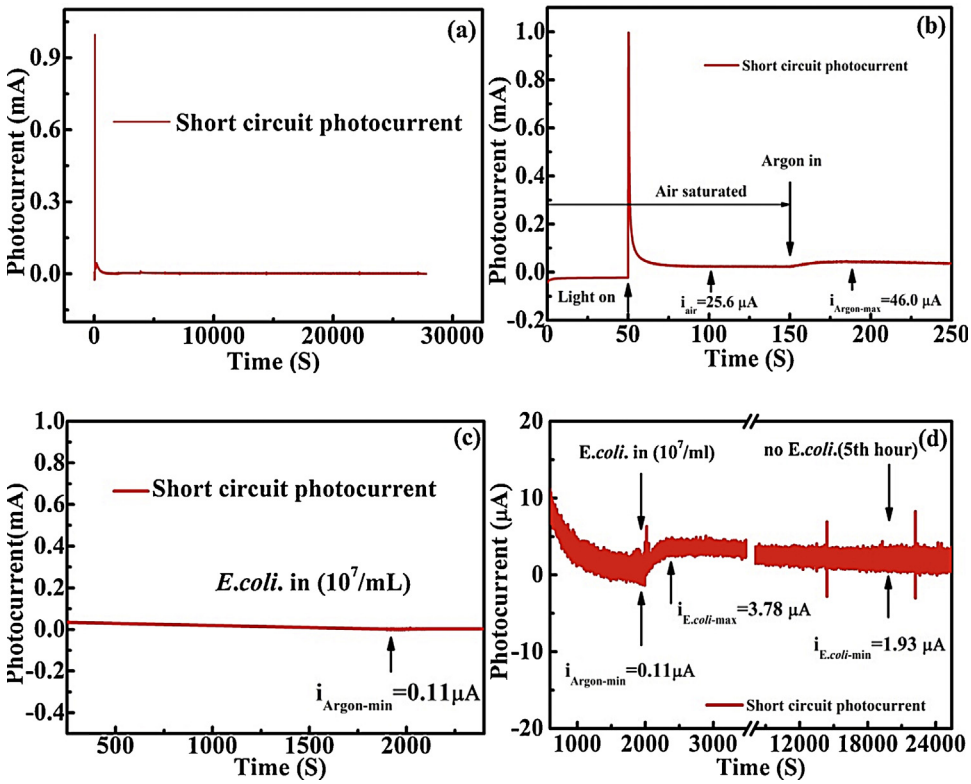

Fig. 7. (a) SCPC measured as the function of time for Cu_2O film electrode in PECMS reactor under different control conditions, (b) enlarged diagram of 0∼250 s, (c) enlarged diagram of 250∼2400 s, and (d) enlarged diagram of 500∼26500 s.

Pt and Ag/AgCl electrodes no toxic and photoactive to *E. coli*. In dark control (Fig. 3b), the bacterial population reduced about 0.5 log, indicating Cu_2O film toxic to *E. coli*. Under VL irradiation (Fig. 3d), about 7 log of *E. coli* can be completely inactivated in 6 h. The results demonstrate Cu_2O film enjoys a good PC inactivation activity.

The PC inactivation activity of Cu_2O film was further confirmed by BacLight kit fluorescent microscopic method [29]. Fig. 4 shows the fluorescence microscopic images of *E. coli*, which is photo-electrocatalytically untreated or treated in the presence of Cu_2O film in PC reactor. Fig. 4a shows the viable cells with intense green fluorescence. After being photoelectrocatalytically treated for 2 h, some cells turned to red fluorescence, indicating some bacteria were cracked and intracellular component was released (Fig. 4b). With prolonged irradiation time, fewer living bacterial cells were observed after 4 and 6 h (Figs. 4c and d), more red stained intracellular DNA and protein came out, indicating that Cu_2O film performed excellent PC inactivation effect.

By contrast, the inactivation efficiency was substantially improved in PEC process (Figs. 3f and e), in which about 7 log of *E. coli* can be completely inactivated within 5 and 2 h by Cu_2O film with a 0 and 0.1 V bias, respectively, further confirming that a bias over flatband potential (−0.35 V) on the n-type Cu_2O film electrode may improve the PEC efficiency and a positive bias on an n-type semiconductor electrode contributes to a highly PEC efficiency. The bactericidal effect was further examined in MS reactor. About 3 log-reduction of *E. coli* in the no Cu_2O cell of MS reactor was observed (Fig. 3c), indicating PC inactivation still worked even no direct contact between *E. coli* and Cu_2O film. Obviously, the inactivation of *E. coli* in the no Cu_2O cell of MS reactor was

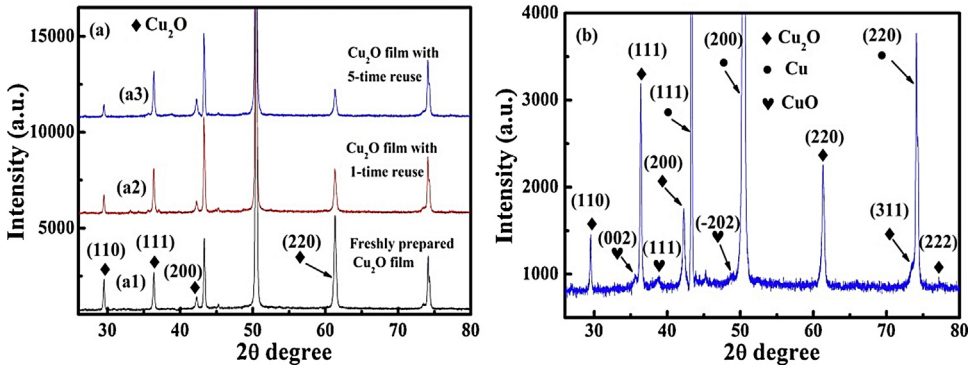

Fig. 8. (a) XRD spectra of (a1) fresh prepared, (a2) 1- and (a3) 5-time reuse Cu_2O films; (b) Enlarged XRD pattern of Fig. 8a(3).

originated from either ROSs or copper ion, both of which were generated in Cu_2O cell and passed through the membrane to the no Cu_2O cell by diffusion.

3.3. The role of ROSs

As we know, electrons and holes generated in a semiconductor when illuminated by light with photoenergy greater than the band gap exhibit high reducing and oxidizing power, respectively. The electron can react with molecular oxygen to produce $^{\bullet}O_2^-$ through a reductive process [30]. The hole can abstract electrons from water and/or hydroxyl ions to generate $^{\bullet}OH$ through an oxidative process [31]. Singlet oxygen ($^1O_2$) is mostly produced indirectly from aqueous reactions of $^{\bullet}O_2^-$ [26]. $^{\bullet}OH$ is a strong and nonselective oxidant [26] that can damage virtually all types of organic biomolecules and $^1O_2$ can irreversibly damage the treated tissues [31]. Consequently, these three types of ROSs ($^{\bullet}OH$, $^{\bullet}O_2^-$, and $^1O_2$) contribute to the major oxidative stress in biological systems [25].

The roles of ROSs are clarified according to the energy levels of Cu_2O and the events possibly occurring during PC processes as well as the testing results for ROSs given in Fig. 5. The band gap of Cu_2O is about 2.0 eV, and the potentials of its conduction band and valence band are −1.4 V and +0.6 V, respectively [32]. Since hole is produced at about +0.6 V, no overpotential is available for the oxidation of water (about +0.57 V, Eq. (1)) [33,34].

$$O_2 + 2H_2O + 4e^- \rightarrow 4OH^- \quad (1)$$

It also cannot oxidize H_2O and OH^- to form H_2O_2 (+1.763 V) and $^{\bullet}OH$ (about +2.8 V), respectively. Indeed, no $^{\bullet}OH$ signal was detected for the intensity of PL signal did not increase with the increasing irradiation time (Fig. 5a). Since hole were not the origin of H_2O_2, electrons were responsible for production of H_2O_2. The production of H_2O_2 could proceed as the cited publication [30] reported: photogenerated electron is likely to react with molecular oxygen to produce $^{\bullet}O_2^-$ (−0.28 V, Eq. (2)), then to H_2O_2 through a reductive process.

$$O_2 + e^- \rightarrow {}^{\bullet}O_2^- \quad (2)$$

However, no $^{\bullet}O_2^-$ signal was detected due to no appearance of absorption peak (470 nm) (Fig. 5b), so $^1O_2$ was not produced [26] and the H_2O_2 came from the direct reduction of O_2 by photogenerated electron (+0.28 V, Eq. (3)), which is more thermodynamically available [35].

$$O_2 + 2H_2O + 2e^- \rightarrow H_2O_2 + 2OH^- \quad (3)$$

Fig. 5c shows the H_2O_2 yield in the MS reactor increased at first and became stable with prolonged irradiation time, due to the decomposition of H_2O_2 in parallel with its production [36]. The equilibrium concentration for H_2O_2 in Cu_2O cell and no Cu_2O cell of MS reactor was estimated to be 7.28 and 2.56 μM, respectively. It is no doubt that no PC process happened in no Cu_2O cell, so the source of supply for H_2O_2 in no Cu_2O cell attributed to diffusion of H_2O_2, which was produced in Cu_2O cell and had a long life span and could pass through the membrane [37]. Note that the total amount of H_2O_2 is much more than actually measured value of 7.28 and 2.56 μM, H_2O_2 was generated continuously and dynamically consumed in situ in the system. Thus, *E. coli* can be inactivated by H_2O_2 in such a low concentration [29,38].

3.4. The role of copper ion

Copper is an essential trace metal required by aquatic microorganisms for their growth [39], but is toxic at high concentration, as it can also bind to biomolecules, such as proteins and nucleic acids, which leads to denaturation and loss of function [40]. In addition, the underlying Fenton-like reactions described as copper-catalyzed Haber-Weiss reactions can produce ROSs to inactivate *E. coli*. The overall reaction for oxidation of Cu(I) in the presence of oxygen can be described as Eq. (4) [41] below:

$$Cu(I) + O_2 \rightarrow ROSs\ (O_2^{\bullet}-,\ H_2O_2, {}^{\bullet}OH) \quad (4)$$

So, copper ion leakage from Cu_2O films may contribute to inactivation of *E. coli*. Fig. 6a shows the variation of copper ion concentration when Cu_2O film immersed in Na_2SO_4 solution under light and dark. The copper ion leakage from Cu_2O film increased fast at first 2 h and slowly later, but with a totally low leakage rate. The concentration of copper ion under dark control was a little less than that under light control, suggesting the n-type Cu_2O film more stable under dark. After 6 h irradiation, 0.536 mg/L of total copper ion were present in Na_2SO_4 solution. The leakage amount of Cu^+ ion was also detected and the final concentration was less than 0.1 mg/L. The low concentration of copper ion leakage from Cu_2O film did not contribute to the antibacterial activity [22]. In order to confirm this, the experiments for the inactivation of *E. coli* in Na_2SO_4 solution with different concentrations of copper ion were carried out. As shown in Fig. 6b, low concentration copper ion (less 2 mg/L) might be nutrient and contribute to bacteria reproduction whereas a high concentration copper ion (over 10 mg/L) was quite the opposite. So, copper ion leakage from Cu_2O film here was not toxic to *E. coli*. In addition, since $^{\bullet}O_2^-$ and $^{\bullet}OH$ were not detected, the copper-catalyzed Haber-Weiss reactions was probably too weak to be observed under current experimental condition.

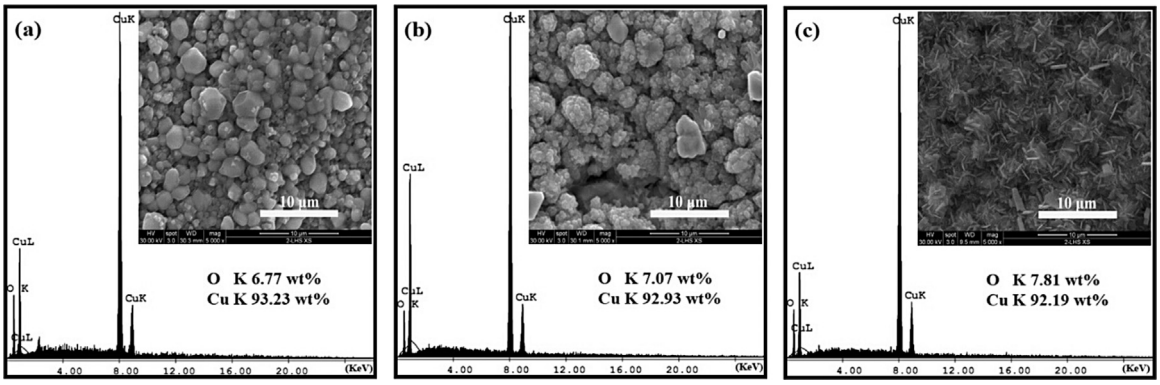

Fig. 9. EDX-SEM patterns and SEM images (insets) of (a) freshly prepared, (b) 1- and (c) 5-time reused Cu_2O films. Each EDX-SEM pattern was obtained based on whole SEM image area.

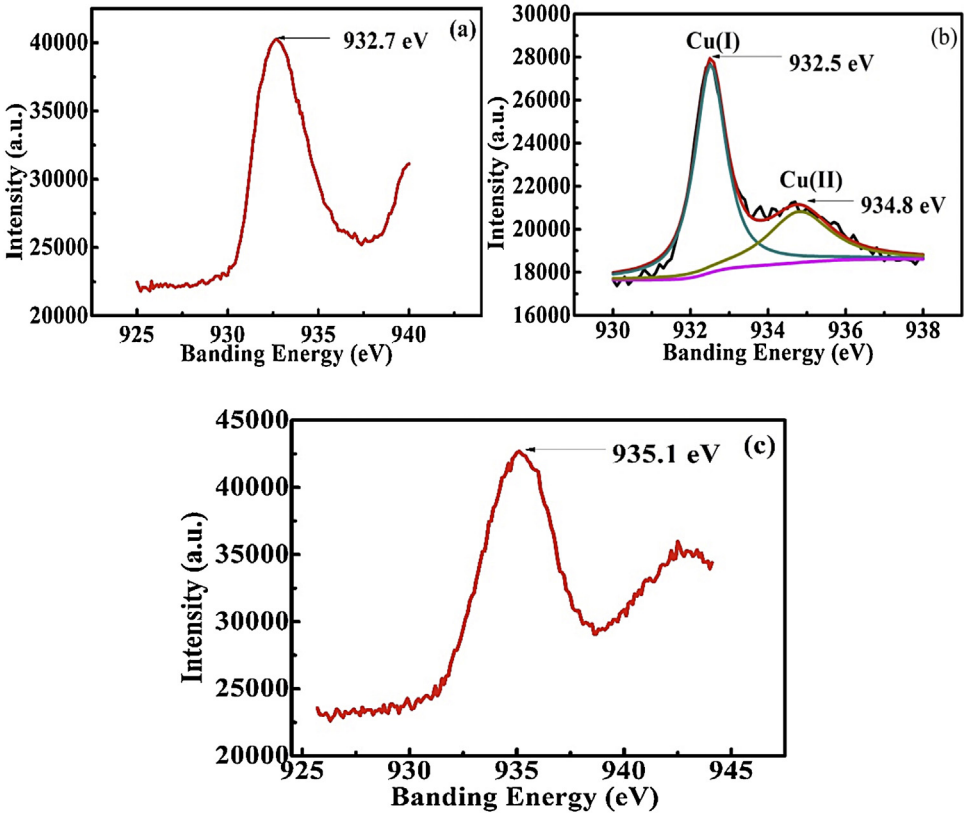

Fig. 10. XPS spectra of freshly prepared (a), 1-time (b) and 5-time reused (c) Cu_2O film.

3.5. The role of electric charge of electrodes

Let's return to the inactivation of *E. coli* in the no Cu_2O cell of MS reactor, which was lower level than that without membrane, indicating the inactivation process was partially inhibited and direct contact between Cu_2O film and *E. coli* was also important during PC process. The results suggest electrons and holes may directly inactivate *E. coli*. In order to confirm this, SCPC was employed to monitor charge transfer between electrodes and *E. coli* in PECMS reactor.

Fig. 7a shows the panorama of SCPC response to different control conditions. Fig. 7b is the enlarged diagram of 0∼250 s part in Fig. 7a. The irradiation began at 50^{th} s. A stable SCPC (i_{air} = 25.6 μA) for Cu_2O film electrode in air-saturated Na_2SO_4 solution was observed. Argon was introduced to bubble the solution at 150^{th} s. Subsequently, the SCPC gradually increased to a maximum 46.0 μA ($i_{Argon\text{-}max}$, Fig. 7b) and eventually reduced to a minimum 0.11 μA ($i_{Argon\text{-}min}$, Fig. 7c). The temporary increase of SCPC contributed to the agitation of solution bubbled by Argon, enhancing the charge transfer between electrodes and solution. Half an hour later, the SCPC reduced to 0.11 μA, which corresponded to the reduction of H^+ to H_2 due to the purge of O_2 dissolved in the solution [2]. At 2000^{th} s, 1 mL of ∼10^8/mL *E. coli* was added to Cu_2O cell of PECMS reactor. It is clear that SCPC quickly increased to a maximum 3.78 μA (Fig. 7d) and then decreased very slowly, indicating electric charge did transfer between Cu_2O film electrode and *E. coli*. However, no any change of SCPC was detected when *E. coli* added into the Pt cell of PECMS reactor (data not shown here), indicating no charge transfer proceeded between Pt electrode and *E. coli*. So, in this case, it is holes, not electrons can be consumed by *E. coli*. Since *E. coli* can capture holes, whether *E. coli* can be inactivated by holes need to be clarified. As shown in Fig. 7d, a complete inactivation of about 7 log *E. coli* was observed in 4.5^{th} h (±0.5 h for deviation in triplicates). It is clear that no ROSs was residual and produced when dissolved O_2 was purged by Argon for over 30 min. So, no ROSs was responsible for the inactivation of *E. coli* in anaerobic condition. In this case, only holes, toxicity of copper ion and Cu_2O film, are possibly involved in the inactivation of *E. coli*. It has been reported that Cu^{2+} can converse to Cu^+ and Cu^+ is more toxic than Cu^{2+} to *E. coli* under anaerobic condition [42]. We determined the total copper ion leakage from Cu_2O film in anaerobic condition with 5 h irradiation was 0.324 mg/L. In order to detect the toxicity of copper ion and Cu_2O film, the inactivation of 7 log *E. coli* by 0.324 mg/L copper ion

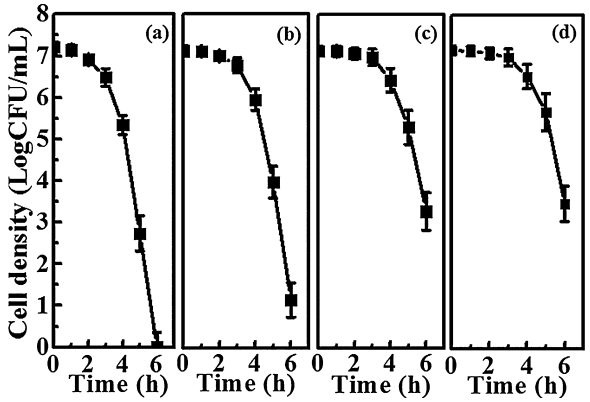

Fig. 11. Photocatalytic inactivation of *E. coli* (about 2×10^7 cfu/mL, 80 mL) by freshly prepared (a), 1-time reused (b), 5-time reused (c), and 10-time reused (d) Cu_2O films in PC reactor.

and Cu_2O film in anaerobic condition was conducted under dark. Fig. S3 shows that about 1.2 log-reduction of *E. coli* were observed in 5 h. So, it is no doubt that besides the toxicity of copper ion and Cu_2O film, holes contributed to the inactivation of *E. coli*. Considering holes produced at about +0.6 V, in this case, the hole can directly inactivate *E. coli* by electrochemically oxidizing co-enzyme A (CoA) in the cell wall to dimeric CoA, resulting in the death of *E. coli* [43].

3.6. Stability and reusability

The stability of Cu_2O film was investigated by comparing the structures, valence states, composition and morphology among freshly prepared, and reused Cu_2O films.

The XRD pattern of the freshly prepared Cu_2O film (Fig. 8a(1)) showed Cu_2O peaks with preferential orientation along (2 2 0) direction, indicating the n-type Cu_2O film synthesized by hydrothermal method have a relatively high percentage of (2 2 0) facets. However, as the increase of reuse times, the diffraction intensity of (2 2 0) plane gradually decreased together with a gradual increase in diffraction intensity of (111) plane (Figs. 8a(1)-(3)), indicating that a prolonged irradiation led to the phase transformation of the n-type Cu_2O film. After 5-time reuse, a weak but new peak (2 2 2) appeared (Fig. 8b), also indicating the phase transformation for the n-type Cu_2O film. The (111) peak became dominant after 5-time reuse, suggesting Cu_2O with dominant (111) plane was more stable than that with other planes under irradiation. Similar results were reported on the phase transformation of p-type Cu_2O by Zheng et al. who concluded that Cu_2O could be used as a stable photocatalyst with exposing (111) facets [19]. Study on crystal face dependence of p-Cu_2O stability as photocathode shows that the (111) surfaces of Cu_2O can be stoichiometrically terminated with Cu^+ against photodecomposition [16]. So, it is expected that the 5-time reused n-type Cu_2O film with highly oriented (111) plane may also be used as a stable photocatalyst. However, we observed the freshly prepared Cu_2O film with brick-red color turned from light black to dark black (See Fig. S1c and S1d) after 1- and 5-time reuse, suggesting a change of phase composition. The enlarged XRD pattern of Fig. 8a(3), which is shown in Fig. 8b, confirmed the change did happen due to the appearance of the three new peaks at $2\theta = 35.60°$, 38.73°and 48.65° corresponding to (0 0 2), (1 1 1) and ($\bar{2}$0 2) planes of tenorite phase CuO (PDF, Powder Diffraction File, No. 02-1040). The diffraction intensity of the CuO peaks was much weaker than that of Cu_2O film, indicating that just a slight change of phase composition happened.

The EDX spectra (Fig. 9) were also suggestive of the oxidation of Cu_2O to CuO for a gradual increase in the oxygen components for the freshly prepared, 1- and 5-time reused Cu_2O films. Considering that copper components (93.23%, 92.93% and 92.19% for the freshly prepared, 1- and 5-time reused Cu_2O films, respectively) were much higher than that (88.81%) for stoichiometric Cu_2O, these Cu_2O films were likely thin in thickness and could be penetrated by the X-ray during the measurement of EDX, so the copper components of Cu_2O films and their copper foil substrates were all included in the process of the measurement, resulting in high copper components in these Cu_2O films. The morphology transformations again suggest the n-type Cu_2O film proceeded a phase transformation and was unstable under irradiation. After 1-time reuse, the morphology of Cu_2O film gradually transformed from stone-like structure (Inset of Fig. 9a) to a mulberry-like one (Inset of Fig. 9b), which finally changed into nanonods and nanosheets (Inset of Fig. 9c) after 5-time reuse.

XPS spectra of the freshly prepared, 1- and 5-time reused Cu_2O films shows the variations of valence states of these films and further confirm the oxidation of Cu_2O to CuO (Fig. 10). The Cu$2p_{3/2}$ level of Cu_2O is narrow (FWHM = 2.0 ± 0.1 eV) and has a binding energy of 933.05 ± 0.75 eV while that of CuO is broad (FWHM = 2.85 ± 0.25 eV) with a binding energy of 935.2 ± 0.35 eV [44]. The peak in Fig. 10a is hard to be simulated since the peak is not so broad and there is no shoulder peak. The binding energy of 932.7 eV for the peak is the same as the standard binding energy of Cu$2p$ in Cu_2O, indicating that the film was prepared as pure Cu_2O, which is well in agreement with the XRD data. The Cu$2p_{3/2}$ spectrum of 1-time reused Cu_2O shows a broad and asymmetry peak simulated with Gaussians fits (Fig. 10b). The binding energy of 932.5 eV and 934.8 eV corresponded to Cu_2O and CuO, respectively, suggesting that surface layer of the Cu_2O film was partly oxidized to CuO after 1-time reuse. However, XRD spectra of 1-time reused Cu_2O film cannot identify the oxidation of Cu_2O to CuO (Fig. 8a(2)), suggesting that the amount of CuO is too low to be detected by the XRD measurement. After 5-time reuse, the Cu$2p_{3/2}$ spectrum (Fig. 10c) presented a peak with binding energy of 935.1 eV corresponding to CuO, indicating the surface layer of Cu_2O was completely oxidized to CuO, which was supported by the XRD data (Fig. 8a(3)). It seems that as the increase of reuse times, more and more Cu_2O was oxidized to CuO. However, no significant change of the XRD pattern, morphology, components was observed for 10-time reused Cu_2O film (data not shown) in comparison with 5-time reused one, indicating that no more Cu_2O was oxidized to CuO after 5-time reuse. The reason is that CuO on surface of Cu_2O can protect Cu_2O from photo-corrosion [45]. The result suggests that despite the n-type Cu_2O with highly oriented (2 2 0) plane unstable under irradiation, it can form a stable compound structure of Cu/Cu_2O/CuO after reuse and may be used as a good photocatalyst.

The reusability of Cu_2O film was investigated by repeated cycling PC tests for bacterial inactivation in PC reactor. A small decrease of inactivation efficiency was observed for 1-time reused Cu_2O film (Figs. 11a and b). However, the inactivation efficiency

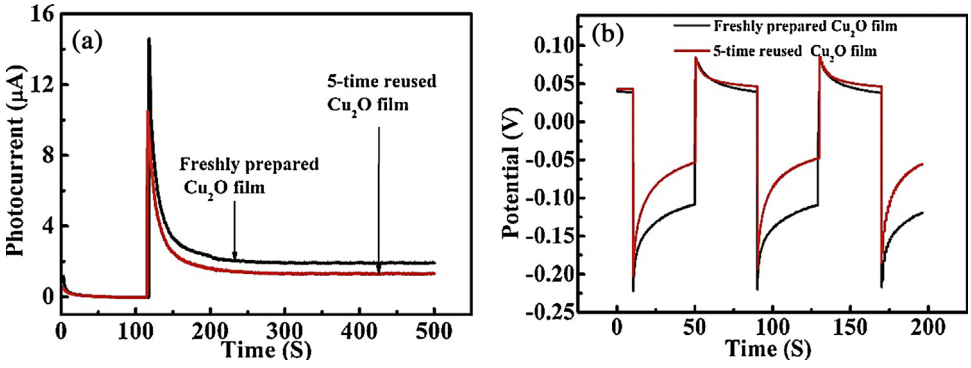

Fig. 12. (a) Short circuit photocurrent, and (b) open circuit photopotential of freshly prepared Cu_2O film and 5-time reused Cu_2O film.

was substantially reduced for 5-time reused Cu_2O film (Fig. 11c) and only about 4 log *E. coli* can be inactivated in 6 h. The decrease of inactivation efficiency was due to the oxidation Cu_2O to CuO. CuO is a semiconductor with a narrow band gap of about 1.4 eV, although it can absorb VL, the PC efficiency is poor due to the serious recombination and the weak redox ability [20]. The result can also be supported by comparing the photoelectrochemical properties between freshly prepared Cu_2O film and 5-time reused Cu_2O film. SCPC (Fig. 12a) and open circuit photopotential (Fig. 12b) were decreased for 5-time reused Cu_2O film in comparison with the freshly prepared Cu_2O film, indicating that the oxidation of Cu_2O to CuO results in the degradation of PC efficiency. Fortunately, no significant differences were observed for SCPC and open circuit photopotential between 5- and 10-time reused Cu_2O films (data not shown here), indicating that $Cu/Cu_2O/CuO$ system became stable after 5-time reuse. The similar inactivation efficiency of 5- and 10-time reused Cu_2O films (Figs. 12c and 12d) further indicates that $Cu/Cu_2O/CuO$ system was stable and available for reuse as a good photocatalyst.

4. CONCLUSIONS

We initiate an investigation on PC and PEC inactivation of *E. coli* by pristine n-type Cu_2O film. 7 log of *E. coli* could be completely inactivated by Cu_2O film within 6 h in a PC process while the bacterial inactivation efficiency was significantly improved in a PEC process, in which 7 log of *E. coli* could be completely inactivated within 2 h by Cu_2O film with a 0.1 V bias. Hole, H_2O_2 and toxicity of Cu_2O film could directly inactivate of *E. coli* and the amount of leakage copper ions (including Cu^{2+} and Cu^{+}) leakage from Cu_2O films was not toxic to *E. coli*. The Cu_2O film was proved to be effective and reusable for PC and PEC inactivation of *E. coli*. The use of PECMS reactor combined with SCPC technique may contribute to the evaluation and mechanism investigation towards PEC disinfection.

ACKNOWLEDGEMENTS

The study was supported by the Research Grants Council of the Hong Kong SAR Government (GRF 477610, GRF 476811) to P.K. Wong; and the National Natural Science Foundation of China (no. 21377044) to Y. Yu. P.K. Wong was also supported by CAS/SAFEA International Partnership Program for Creative Research Teams of Chinese Academy of Sciences, China.

Appendix A. Supplementary data

Supplementary data associated with this article can be found, in the online version, at http://dx.doi.org/10.1016/j.electacta.2014.11.169.

REFERENCES

[1] L. Xiong, S. Huang, X. Yang, M. Qiu, Z. Chen, Y. Yu, p-Type and n-type Cu_2O semiconductor thin films: Controllable preparation by simple solvothermal method and photoelectrochemical properties, Electrochim. Acta 56 (2011) 2735.
[2] C.M. McShane, K.-S. Choi, Photocurrent enhancement of n-type Cu_2O electrodes achieved by controlling dendritic branching growth, J. Am. Chem. Soc. 131 (2009) 2561.
[3] G. Hodes, I.D.J. Howell, L.M. Peter, Nanocrystalline photoelectrochemical cells: A new concept in photovoltaic cells, J. Electrochem. Soc. 139 (1992) 3136.
[4] J.J. Cooney, R.-J. Tang, Quantifying effects of antifouling paints on microbial biofilm formation, in: J.D. Ron (Ed.), Methods in Enzymology, Academic Press, 1999, pp. 637.
[5] J. Ren, W. Wang, S. Sun, L. Zhang, L. Wang, J. Chang, Crystallography facet-dependent antibacterial activity: The case of Cu_2O, Ind. Eng. Chem. Res. 50 (2011) 10366.
[6] H. Pang, F. Gao, Q. Lu, Morphology effect on antibacterial activity of cuprous oxide, Chem. Commun. (2009) 1076.
[7] Y. Wang, G. She, H. Xu, Y. Liu, L. Mu, W. Shi, Cu_2O nanoparticles sensitized ZnO nanorod arrays: Electrochemical synthesis and photocatalytic properties, Mater. Lett. 67 (2012) 110.
[8] W. Zhao, K.-H. Wong, C. Hu, J.C. Yu, C.Y. Chan, T. Qi, P.K. Wong, Synthesize of Cu_2O-CuO/$Sr_3BiO_{5.4}$ and its photocatalytic activity, Appl. Surf. Sci. 258 (2012) 5955.
[9] Q. Zhu, Y. Zhang, F. Wu, D. Tan, P. Wang, P.K. Chu, Mineral wool fibers incorporated with cuprous oxide for visible light photocatalytic inactivation of *Escherichia coli*, Ceram. Int. 40 (2014) 5407.
[10] S. Zhang, C. Liu, X. Liu, H. Zhang, P. Liu, S. Zhang, F. Peng, H. Zhao, Nanocrystal Cu_2O-loaded TiO_2 nanotube array films as high-performance visible-light bactericidal photocatalyst, Appl. Microbiol. Biotechnol. 96 (2012) 1201.
[11] L.W. Yan, L.B. Xiong, J.L. Li, H.Y. Yip, P.K. Wong, Y. Yu, Preparation and photocatalytic sterilization property of Cu_2O nanostructure with copper anode oxidation method, Chinese J. Inorg. Chem. 11 (2009) 1960.
[12] T. Matsunaga, Y. Namba, T. Nakajima, Electrochemical sterilization of microbial cells, Bioelectrochem. Bioenerg. 13 (1984) 393.
[13] T. Matsunaga, R. Tomoda, T. Nakajima, H. Wake, Photoelectrochemical sterilization of microbial cells by semiconductor powders, FEMS Microbiol. Lett. 29 (1985) 211.
[14] A. Paracchino, N. Mathews, T. Hisatomi, M. Stefik, S.D. Tilley, M. Grätzel, Ultrathin films on copper(I) oxide water splitting photocathodes: a study on performance and stability, Energy Environ. Sci. 5 (2012) 8673.
[15] L. Wu, L. Tsui, N. Swami, G. Zangari, Photoelectrochemical stability of electrodeposited Cu_2O films, J. Phys. Chem. C 114 (2010) 11551.
[16] K.L. Sowers, A. Fillinger, Crystal face dependence of p-Cu_2O stability as photocathode, J. Electrochem. Soc. 156 (2009) F80.
[17] M.J. Siegfried, K.-S. Choi, Elucidating the effect of additives on the growth and stability of Cu_2O surfaces via shape transformation of pre-grown crystals, J. Am. Chem. Soc. 128 (2006) 10356.
[18] Q. Hua, D. Shang, W. Zhang, K. Chen, S. Chang, Y. Ma, Z. Jiang, J. Yang, W. Huang, Morphological evolution of Cu_2O nanocrystals in an acid solution: Stability of different crystal planes, Langmuir 27 (2011) 665.
[19] Z. Zheng, B. Huang, Z. Wang, M. Guo, X. Qin, X. Zhang, P. Wang, Y. Dai, Crystal faces of Cu_2O and their stabilities in photocatalytic reactions, J. Phys. Chem. C 113 (2009) 14448.
[20] L. Huang, F. Peng, H. Yu, H. Wang, Preparation of cuprous oxides with different sizes and their behaviors of adsorption, visible-light driven photocatalysis and photocorrosion, Solid State Sci. 11 (2009) 129.
[21] L.S. Zhang, K.-H. Wong, D.Q. Zhang, C. Hu, J.C. Yu, C.Y. Chan, P.K. Wong, Zn:In $(OH)_yS_z$ solid solution nanoplates: Synthesis, characterization, and photocatalytic mechanism, Environ. Sci. Technol. 43 (2009) 7883.
[22] K. Sunada, M. Minoshima, K. Hashimoto, Highly efficient antiviral and antibacterial activities of solid-state cuprous compounds, J. Hazard. Mater. 235–236 (2012) 265.
[23] K. Ishibashi, A. Fujishima, T. Watanabe, K. Hashimoto, Quantum yields of active oxidative species formed on TiO_2 photocatalyst, J.Photochem. Photobiol. A: Chem 134 (2000) 139.
[24] B.A.L. Mark, W. Sutherland, The tetrazolium dyes MTS and XTT provide new quantitative assays for superoxide and superoxide dismutase, Free Radical Res. 27 (1997) 283.
[25] Y. Li, W. Zhang, J. Niu, Y. Chen, Mechanism of photogenerated reactive oxygen species and correlation with the antibacterial properties of engineered metal-oxide nanoparticles, ACS Nano 6 (2012) 5164.
[26] L. Brunet, D.Y. Lyon, E.M. Hotze, P.J.J. Alvarez, M.R. Wiesner, Comparative photoactivity and antibacterial properties of C_{60} fullerenes and titanium dioxide nanoparticles, Environ. Sci. Technol. 43 (2009) 4355.
[27] H. Bader, V. Sturzenegger, J. Hoigné, Photometric method for the determination of low concentrations of hydrogen peroxide by the peroxidase catalyzed oxidation of N,N-diethyl-*p*-phenylenediamine (DPD), Water Res. 22 (1988) 1109.
[28] W. Wang, Y. Yu, T. An, G. Li, H.Y. Yip, J.C. Yu, P.K. Wong, Visible-light-driven photocatalytic inactivation of *E. coli* K-12 by bismuth vanadate nanotubes: Bactericidal performance and mechanism, Environ. Sci. Technol. 46 (2012) 4599.
[29] D. Xia, T.W. Ng, T. An, G. Li, Y. Li, H.Y. Yip, H. Zhao, A. Lu, P.K. Wong, A recyclable mineral catalyst for visible-light-driven photocatalytic inactivation of bacteria: Natural magnetic sphalerite, Environ. Sci. Technol. 47 (2013) 11166.
[30] H. Lin, S. Liao, S. Hung, The dc thermal plasma synthesis of ZnO nanoparticles for visible-light photocatalyst, J. Photochem. Photobiol. A: Chem. 174 (2005) 82.
[31] S. Wang, R. Gao, F. Zhou, M. Selke, Nanomaterials and singlet oxygen photosensitizers: Potential applications in photodynamic therapy, J. Mater. Chem. 14 (2004) 487.
[32] L. Xiong, M. Ouyang, L. Yan, J. Li, M. Qiu, Y. Yu, Visible-light energy storage by Ti^{3+} in TiO_2/Cu_2O bilayer film, Chem. Lett. 38 (2009) 1154.
[33] P.E. de Jongh, D. Vanmaekelbergh, J.J. Kelly, Photoelectrochemistry of electrodeposited Cu_2O, J. Electrochem Soc. 147 (2000) 486.
[34] P.E. de Jongh, D. Vanmaekelbergh, J.J. Kelly, Cu_2O: A catalyst for the photochemical decomposition of water? Chem. Commun. (1999) 1069.
[35] Y. Chen, A. Lu, Y. Li, L. Zhang, H.Y. Yip, H. Zhao, T. An, P.K. Wong, Naturally occurring sphalerite as a novel cost-effective photocatalyst for bacterial disinfection under visible light, Environ. Sci. Technol. 45 (2011) 5689.
[36] F. Shiraishi, C. Kawanishi, Effect of diffusional film on formation of hydrogen peroxide in photocatalytic reactions, J.Phys. Chem. A 108 (2004) 10491.

[37] A. Rincon, Effect of pH, inorganic ions, organic matter and H_2O_2 on *E. coli* K12 photocatalytic inactivation by TiO_2 Implications in solar water disinfection, Appl. Catal. B: Environ. 51 (2004) 283.
[38] W. Wang, L. Zhang, T. An, G. Li, H. Yip, P. Wong, Comparative study of visible-light-driven photocatalytic mechanisms of dye decolorization and bacterial disinfection by B-Ni-codoped TiO_2 microspheres: The role of different reactive species, Appl. Catal. B: Environ. 108–109 (2011) 108.
[39] W.G. Sunda, Trace metal interactions with marine phytoplankton, Biol. Oceanogr. 6 (1989) 411.
[40] R.B. Thurman, C.P. Gerba, G. Bitton, The molecular mechanisms of copper and silver ion disinfection of bacteria and viruses, Crit. Rev. Environ. Control 18 (1989) 295.
[41] N. Perez-Almeida, M. Gonzalez-Davila, J.M. Santana-Casiano, A.G. Gonzalez, M. Suarez de Tangil, Oxidation of Cu(I) in seawater at low oxygen concentrations, Environ. Sci. Technol. 47 (2013) 1239.
[42] P.H. Beswick, G.H. Hall, A.J. Hook, K. Little, D.C. McBrien, K.A. Lott, Copper toxicity: evidence for the conversion of cupric to cuprous copper *in vivo* under anaerobic conditions, Chem. Biol. Interact. 14 (1976) 347.
[43] T. Matsunaga, Y. Namba, T. Nakajima, Electrochemical sterilization of microbial cells, Bioelectrochem. Bioenerg. 13 (1984) 393.
[44] T. Ghodselahi, M.A. Vesaghi, A. Shafiekhani, A. Baghizadeh, M. Lameii, XPS study of the Cu@Cu_2O core-shell nanoparticles, Appl. Surf. Sci. 255 (2008) 2730.
[45] K. Borgohain, N. Murase, S. Mahamuni, Synthesis and properties of Cu_2O quantum particles, J. Appl. Phys. 92 (2002) 1292.